Octupole deformation in ^{227}Ac by single-proton stripping reactions: ^{226}Ra(α, t)^{227}Ac and ^{226}Ra(^{3}He,d)^{227}Ac

H. E. Martz* and R. K. Sheline†
Nuclear Chemistry Division, Lawrence Livermore National Laboratory, Livermore, California 94550 and Florida State University, Tallahassee, Florida 32306

R. G. Lanier, R. W. Hoff, G. L. Struble, and D. J. Decman
Nuclear Chemistry Division, Lawrence Livermore National Laboratory, Livermore, California 94550

D. G. Burke
McMaster University, Hamilton, Ontario, Canada

R. R. Chasman
Department of Physics, Argonne National Laboratory, Argonne, Illinois 68439

R. A. Naumann
Department of Physics, Princeton University, Princeton, New Jersey 08544
(Received 30 October 1987)

A radioactive ^{226}Ra ($t_{1/2}=1600$ yr) target was used to study the ^{226}Ra(α,t)^{227}Ac and ^{226}Ra(^{3}He,d)^{227}Ac reactions at an incident energy of 30 MeV for both the α and ^{3}He particles. These measurements have confirmed most levels observed in earlier decay-scheme studies, and give evidence for 11 additional levels. Several of the new levels were used in the tentative assignment of two $K^\pi=\frac{5}{2}^\pm$ bands. The experimental data are compared with results from the Nilsson model and a nonadiabatic, rigid, reflection-asymmetric rotor (octupole) model. Although the order and spacing of levels in this mass region can be explained better by models that include an octupole deformation, the spectroscopic strengths in ^{227}Ac are in better agreement with those calculated for the reflection-symmetric potential.

I. INTRODUCTION

When very low-lying negative-parity states were discovered in the radium region[1] during the mid 50s, the possibility of nuclei having stable octupole deformation was considered.[2] In the region of nuclei just beyond the double-closed shells of ^{208}Pb, the $g_{9/2}$ and $j_{15/2}$ neutron levels and the $f_{7/2}$ and $i_{13/2}$ proton levels are energetically very close together. Couplings among these orbitals give rise to low-energy $I^\pi=3^-$ two-quasiparticle configurations, and a superposition of these configurations could form the microscopic basis for stable octupole deformations.[3]

In 1980 one of us showed[4] that incipient octupole deformation effects give rise to parity doublets in many odd nuclides of this mass region, including ^{227}Ac. Subsequently, Möller and Nix[5] calculated a minimum in the nuclear potential-energy surface for nonzero octupole deformation. The lowering of the ground-state energy due to additional stability coming from octupole deformation improved the agreement between calculated and experimental masses in the region around ^{222}Ra. More recently, several other calculations[6-8] have confirmed this minimum in the potential energy surface.

Leander and Sheline[9] have developed a model with either strong or intermediate coupling which takes into explicit account the parity decoupling and tested its predictions against a number of odd-A nuclides, including ^{227}Ac.

Using a Skyrme III interaction in a Hartree-Fock plus BCS approximation, Bonche *et al.*[10] obtained a potential minimum at nonzero octupole deformation for ^{222}Ra. The minimum from calculations by Nazarewicz[7] that used a beta parametrization and from calculations by Chasman[11] that included 2^6 pole deformation showed a somewhat smaller lowering of the ground-state energy due to octupole deformation. A shallow minimum might imply the breakdown of a mean-field description of octupole deformation.

These theoretical studies have inspired experimental searches for stable octupole deformation in the mass region $220<A<230$ even though target materials are unstable and radioactive sources have short half-lives. The first experimental confirmation of octupole deformation came from the observation[12] of the predicted[4] ground-state parity doublet in ^{229}Pa. This was soon followed by the study of ^{227}Ac.[13]

In addition to parity doublets, the different parity states of $K=\frac{1}{2}^\pm$ bands are expected to have decoupling parameters with the same absolute value but with opposite sign in the static octupole deformation limit.[9,13,14] Other predictions of a static octupole picture are (1) the

magnetic moments of parity doublet states are identical,[9] (2) $E1$ and $E3$ transition rates are enhanced in such bands,[9] and (3) reduced alpha-decay rates to both members of a parity doublet are identical.[9] In many-body calculations,[4] there is a separate solution for each value of the parity. One finds here a tendency for the two decoupling parameters to approach each other in magnitude, but there is seldom the equality that is characteristic of the static picture. In this picture, one also expects to see relatively larger differences in the α-decay hindrance factors to the positive and negative parity band members for even nuclides in comparison to odd nuclides.[9]

In this paper ^{227}Ac has been studied with reaction spectroscopy to further test the picture of static octupole deformation in this nucleus. Earlier work on ^{227}Ac is summarized in the nuclear data compilation of Maples.[15] Subsequently, Teoh *et al.*[16] and Aniĉin *et al.*[17] performed additional decay-scheme experiments. With information combined from these studies, three rotational bands have been assigned in ^{227}Ac (Refs. 15–17): a $\frac{3}{2}^-$ ground-state band, a $\frac{3}{2}^+$ band at 27.37 keV, and a decoupled $K^\pi=\frac{1}{2}^-$ band where the lowest level at 330.02 keV has $I=\frac{3}{2}$. Sheline and Leander[13] recently reinterpreted the decay-scheme data and provided evidence for an additional $K^\pi=\frac{1}{2}^+$ band starting with a $\frac{5}{2}^+$ level at 425.65 keV. In their paper they point out that the approximately degenerate $K^\pi=\frac{3}{2}^\pm$ bands approach closely the properties expected for a stable octupole-deformed core. However, the experimental energies and decoupling parameters of the $K^\pi=\frac{1}{2}^\pm$ bands differ from the values predicted by the limit of a stable octupole shape (strong coupling) and instead are characteristic of a weak coupling to the octupole-deformed core of the reflection symmetric $\frac{1}{2}^-[530]$ and $\frac{1}{2}^+[660]$ Nilsson orbitals.

By contrast, the α decay of ^{231}Pa into both bands of the proposed $\frac{1}{2}^\pm$ parity doublet in ^{227}Ac shows[9] that the parity-changing α transitions are reasonably favored (HF=15) relative to the natural-parity transitions (HF=1). Remembering that for reflection symmetric deformed actinides, favored α transitions occur between similar intrinsic configurations (in odd-A nuclei from the parent ground state to the band of the same single-particle state in the daughter), these results seem to suggest that the parity doublet is related to a single, intrinsic configuration. Opposite parity states in odd-A nuclei in the region around $A=240$ routinely have hindrance-factor ratios of several thousand, when one state is allowed and the other is not. Thus, it is still an open question whether the $K^\pi=\frac{1}{2}^\pm$ parity doublet in ^{227}Ac results from a static octupole deformation.

A measurement of the $E1$ transition rate between the $\frac{3}{2}^+$ and $\frac{3}{2}^-$ ground-state doublet in ^{227}Ac shows that there is no enhancement of the $E1$ rate, as predicted and observed in other nuclei in this region.[18] On the other hand, the magnetic moments for the $\frac{3}{2}^+$ and $\frac{3}{2}^-$ parity doublet at and near the ground state in ^{227}Ac have been shown within experimental limits to be identical.[13]

Until quite recently, the theoretical treatment of the low-lying spectrum of ^{227}Ac has been based on the use of the Nilsson orbitals $\frac{3}{2}^-[532]$, $\frac{3}{2}^+[651]$, and $\frac{1}{2}^-[530]$, which assumes that the nucleus has only a prolate deformation. It is, however, very difficult to reproduce the Nilsson level order with a simple prolate potential. Furthermore, magnetic moments and decoupling parameters generally disagree with the Nilsson model predictions.

In the present work, spectroscopic strengths of ^{227}Ac levels populated by single-proton stripping reactions were examined to provide an additional test for the presence of static octupole deformation. It is well known[19] that for such reactions the cross sections to the various members of a rotational band in an odd-A nucleus are directly proportional to the corresponding "shell model" amplitudes in the intrinsic state on which the band is based. Therefore, in principle, it is possible to determine these amplitudes from the experimental cross sections (subject to uncertainties introduced due to incomplete knowledge of the reaction process, etc.). In particular, for certain intrinsic states, it might be expected that the wave function amplitudes, and hence the corresponding experimental cross sections, could be changed significantly by the presence of an octupole deformation. For example, in the absence of an octupole shape, the lowest positive-parity band in ^{227}Ac would be interpreted as the $\frac{3}{2}^+[651]$ Nilsson orbital, which originates from the $i_{13/2}$ shell-model state and therefore has a large amplitude $|C_{jl}|$ for $j=\frac{3}{2}$. Calculations by Chasman[20] predict a value of $C_{jl}^2=0.75$ for $j=\frac{13}{2}$ if the octupole deformation is $\beta_3=0$. However, $C_{jl}^2=0.15$ for $\beta_3=0.1$, a value considered likely in this region.[9] The measurements described in this paper were undertaken in the hope of exploiting such differences in C_{jl} values to test for the presence of a static octupole deformation.

II. EXPERIMENT

A. Data acquisition and results

The ^{226}Ra(α,t)^{227}Ac and ^{226}Ra(^{3}He,d)^{227}Ac reactions were performed at the McMaster University Tandem Accelerator Laboratory. In separate experiments, beams of α particles and ^{3}He particles were accelerated to an energy of 30 MeV and were focused onto a radioactive ^{226}Ra ($t_{1/2}=1600$ yr) target. The target was supported by a carbon backing, and from elastic scattering yields, the thickness of radium was estimated to be ~ 40 μg/cm^2. The tritons and deuterons emitted during the reactions were momentum analyzed by an Enge split-pole magnetic spectrometer and detected by nuclear-emulsion plates mounted in the focal plane of the magnet. The target was irradiated in the first set of experiments by an ~ 325 nA α-particle beam for an average of ~ 12 h per spectrometer angle. In the second set of experiments, the same target was irradiated by an ~ 510 nA ^{3}He beam for an average of ~ 12 h per angle. Data were collected at angles of 40°, 60°, and 70° for the (α,t) reaction, and at angles of 27,5°, 45°, 70°, and 75° for the (^{3}He,d) reaction. The angles were chosen so that particle groups from light impurities would be kinematically removed from the regions of excitation energy that were of interest.

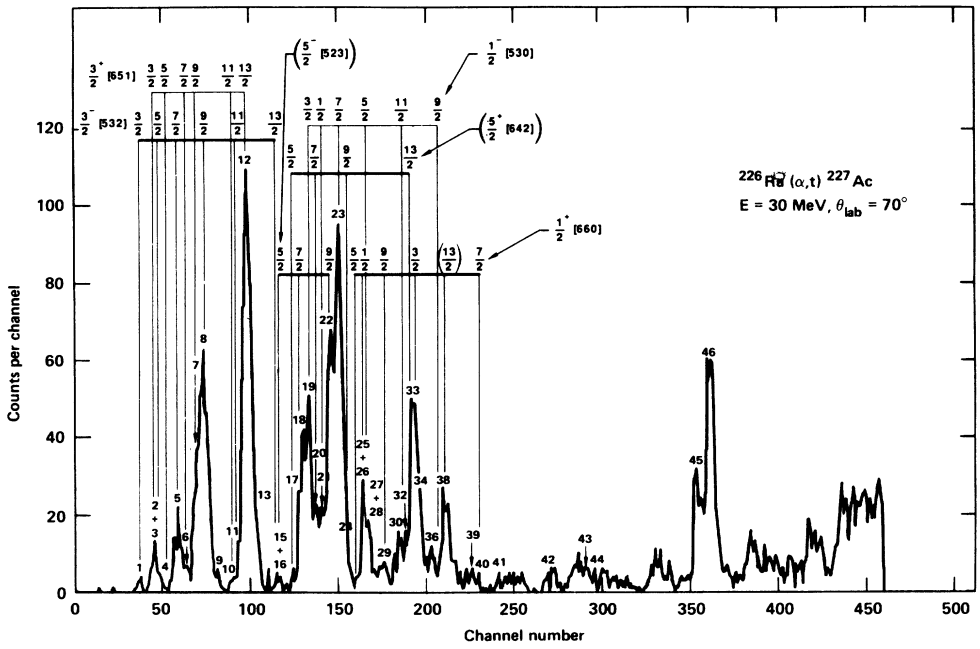

FIG. 1. Spectrum from the ^{226}Ra(α,t)^{227}Ac reaction. The peaks are labeled to correspond with energies quoted in Table I. The Nilsson quantum numbers shown without parentheses indicate previously assigned bands (Ref. 13). Those with parentheses are tentative assignments made in the present work.

The 70° spectra for the ^{226}Ra(α,t)^{227}Ac and the ^{226}Ra(^{3}He,d)^{227}Ac reactions are shown in Figs. 1 and 2. The energy resolution in the experiments ranged between 14–16 keV for the (α,t) runs and between 21–22 keV for the (^{3}He,d) runs. A summary of these results is presented in Table I. Excitation energies were determined from a spectrograph calibration obtained separately using α particles from a ^{212}Pb source. The uncertainties on the excitation energies are <2 keV in the most favorable cases of large resolved peaks, but are greater for weak or poorly resolved peaks. The reaction yield data measured in the spectrograph at different angles were normalized to the number of elastic-scattering events counted (with appropriate dead-time corrections) in a solid-state monitor detector placed at 29.5° with respect to the beam. Absolute cross sections were derived by normalizing the monitor elastic yields to distorted wave Born approximation (DWBA) calculations[21] of the elastic-scattering cross section, using the known ratio of the monitor and spectrometer solid angles. Optical-model potentials for the DWBA calculations were the same as those used by Elze.[22]

In the present, studies levels populated in the single-proton stripping reactions are often separated by only a few keV; thus, a spectrum-stripping program[23] was used to extract excitation energies and intensities from the data. The complexity of the spectrum precluded the normal search-find-fit technique which would generally be applicable in a well-resolved spectrum with isolated peaks. Therefore, to analyze each spectrum, peaks were fixed at positions corresponding to well-known energy levels[15–17] in ^{227}Ac. The analysis was started by constraining peak positions for a region containing a fairly well-resolved and isolated-peak group (e.g., group number 12 in Fig. 1). A symmetrical Gaussian peak shape was used, and the width parameter, σ, was obtained by a best-fit procedure that allowed σ and the peak intensities to vary. The remainder of the spectrum was then analyzed with this value of σ, with fixed-position peak groups being removed or variable-position peak groups being added one at a time as necessary to obtain the best fit.

As an example, Fig. 3 shows a region of the (α,t) spectrum taken at 70° and centered about $\sim$350 keV [see Fig. 3(a)]. Simply using the known levels does not give a good representation of the data [see Fig. 3(b)], but by judiciously adding a reasonable number of new peaks [see Fig. 3(c)], a good fit is achieved. In particular, it is clear that new levels are needed at 316 and 372 keV [labeled as peaks 18 and 22 in Fig. 3(c)]. The credibility of this procedure is strengthened by the fact that similar results were obtained consistently from the (α,t) spectra at different angles. In the (^{3}He,d) spectra, however, the resolution was significantly poorer, and the results of this type of analysis were more ambiguous.

Because the preparation of the target involved chemical purifications,[24] there were concerns that any heavy mass contaminants would add spurious low-intensity peaks to the spectra. These would not necessarily be easily identified because they would have a relatively small kinematic shift and might be obscured by statistical fluctuations in the fitting procedure. Therefore, ^{226}Ra(p,p')

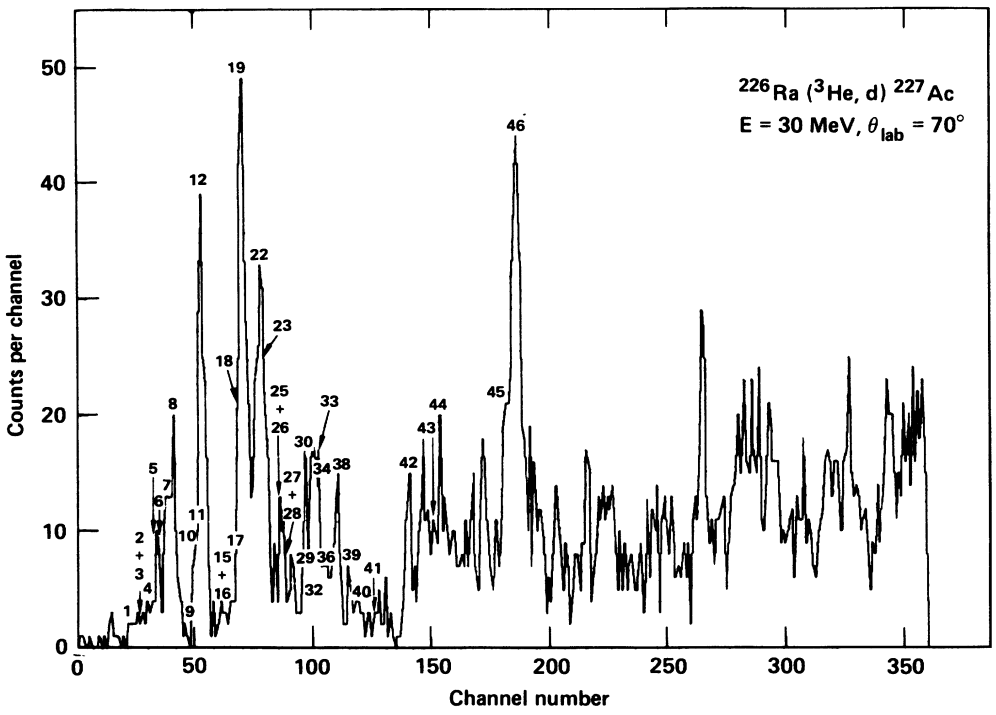

FIG. 2. Spectrum from the ^{226}Ra(^{3}He,d)^{227}Ac reaction. The peaks are labeled to correspond with the energies quoted in Table I.

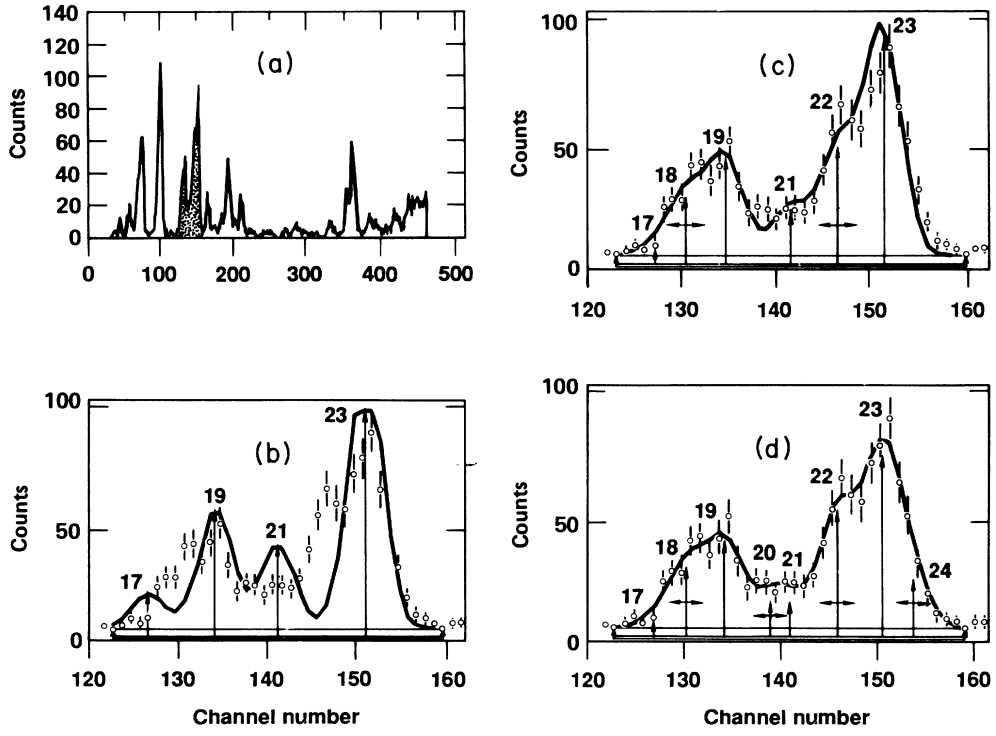

FIG. 3. Deconvolution of the (α,t) spectra data: An illustrated example. (a) The full spectrum (Fig. 1) with the shaded area noting the complex peak group at ~350 keV to be fit. (b) The fit when peaks corresponding only to known energies are inserted (see Table I). (c) The fit with peaks 18 and 22 added. (d) The final fit when peaks 20 and 24 are also added. For this spectrum, the peak width parameter (FWHM) was determined to be 15 keV using peak group 12 as discussed in text. In the fit illustrated here, this parameter was held constant in fitting the remaining peaks in the spectrum.

TABLE I. Summary of results from the ^{226}Ra(α,t) and ^{226}Ra(^{3}He,d) reactions. The numbers in column 1 correspond to peaks labeled in Figs. 1 and 2.

Level	Energy (keV) Lit.[a] Value	This work[b] (α,t)	(^{3}He,d)	Intensity (counts) at 70° (α,t)[c]	(^{3}He,d)[c]	Nilsson model interpretation[f] $IK^{\pi}[Nn_z\Lambda]$
1	0	0	0	16	8	$\frac{3}{2}\frac{3}{2}^-$[532]
2	27.37	30	27	49	12	$\frac{3}{2}\frac{3}{2}^+$[651]
3	29.98					$\frac{5}{2}\frac{3}{2}^-$[532]
4	46.35	46	46	10	14	$\frac{5}{2}\frac{3}{2}^+$[651]
5	74.13	74	74	78	16	$\frac{7}{2}\frac{3}{2}^-$[532]
6	84.55	85	85	26	18	$\frac{7}{2}\frac{3}{2}^+$[651]
7	109.96	110	110	120	38	$\frac{9}{2}\frac{3}{2}^+$[651]
8	126.85	127	127	324	50	$\frac{9}{2}\frac{3}{2}^-$[532]
9	(160)	(148±5)	(160±5)	26	<9	
10	187.34	187	187	30	16	$\frac{11}{2}\frac{3}{2}^+$[651]
11	198.67	199	199	19	27	$\frac{11}{2}\frac{3}{2}^-$[532]
12	210.81	211	211	517	109	$\frac{13}{2}\frac{3}{2}^+$[651]
13		227±2		89	<10	
14		(249±2)[d]	(244±5)[e]	<10		
15	271.33	272	272	18	13	$\frac{13}{2}\frac{3}{2}^-$[532]
16	273.13					($\frac{5}{2}\frac{5}{2}^-$[523])
17	304.6	305	305	25	27	($\frac{5}{2}\frac{5}{2}^+$[642])[g]
18		316±2	320±5	141	67	($\frac{7}{2}\frac{5}{2}^-$[523])
19	330.02	330	330	186	166	$\frac{3}{2}\frac{1}{2}^-$[530]
20		342±5		59		($\frac{7}{2}\frac{5}{2}^+$[642])
21	354.59	355		56		$\frac{1}{2}\frac{1}{2}^-$[530]
22		372±2	377±6	260	92	($\frac{9}{2}\frac{5}{2}^-$[523])
23	387.12	387	387	372	75	$\frac{7}{2}\frac{1}{2}^-$[530]
24		403±5	404±5	99	<10	($\frac{9}{2}\frac{5}{2}^+$[642])

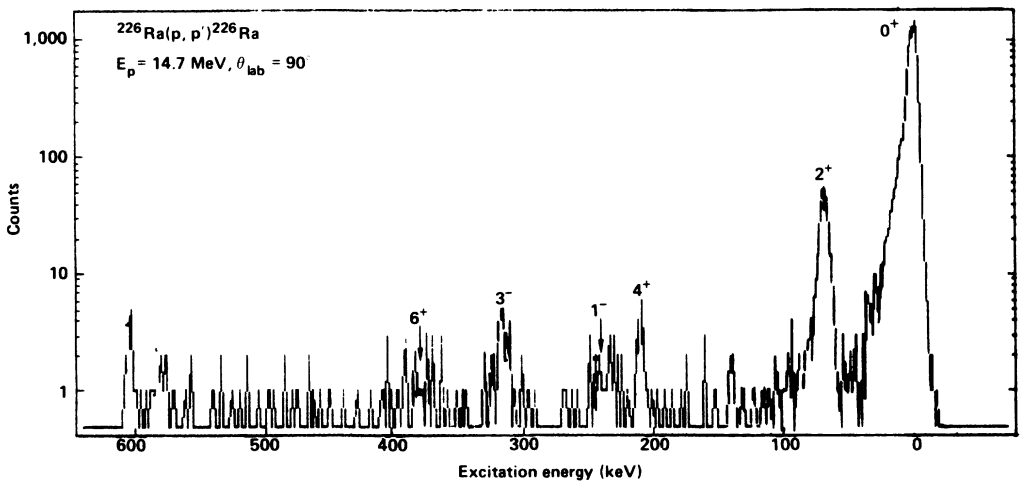

FIG. 4. Spectrum from the ^{226}Ra(p,p') reaction. The peak groups correspond to well-known states (Ref. 25) in ^{226}Ra and are labeled with their appropriate spins and parities.

TABLE I. (*Continued*).

Level	Energy (keV) Lit.[a] Value	Energy (keV) This work[b] (α,t)	Energy (keV) This work[b] (^{3}He,d)	Intensity (counts) at 70° (α,t)[c]	Intensity (counts) at 70° (^{3}He,d)[c]	Nilsson model interpretation[f] $IK^{\pi}[Nn_z\Lambda]$
25	425.65	428	427	14	35	$\frac{5}{2}\frac{1}{2}^+[660]$
26	(428.4)					
27	(435.4)	438	437	104	30	$\frac{1}{2}\frac{1}{2}^+[660]$
28	438.0					$\frac{5}{2}\frac{1}{2}^-[530]$
29	469.2	469	469	30	14	$\frac{9}{2}\frac{1}{2}^+[660]$
30	501.3	501	501	58	25	
31	(508.9)					$\frac{11}{2}\frac{1}{2}^-[530]$
32	515.2	515	515	27	7	
33		528±3	523±8	138	26	$(\frac{13}{2}\frac{5}{2}^+[642])$
34	537.2	537	537	173	37	$\frac{3}{2}\frac{1}{2}^+[660]$
35		549±3		<10		
36	563.0	563	563	45	16	
37	(576.6)	577[d]				$\frac{9}{2}\frac{1}{2}^-[530]$
38		593±2	589±3	111	42	$(\frac{13}{2}\frac{1}{2}^+[660])$
39	(639.1)	639	639	20	9	
40	656.3	657	657	10	8	
41	(698.5)	698	698	7	8	
42	(790.0)	790	790	8	29	
43	(863.6)	864	860	22	21	
44	(874.7)	875	875	11	30	
45		1068±2	1068±5	124	65	
46		1091±2	1093±4	277	147	

[a]The energies are average values obtained from the results quoted in Refs. 15–17. Entries given in parentheses are less certain because there is only tentative evidence for the level or because the level was observed only on one previous experiment.

[b]All known levels were fixed in the spectrum (see text) to ±1 keV. Individual levels separated by less than ~5 keV could not be meaningfully isolated by the fitting procedure (note curly brackets in column 2). For such cases, energies represent the center of gravity of the multiplet. New levels are quoted with their calculated statistical uncertainties and with weighted average energies based on results from two or more angles. Parentheses indicate that substantially weaker evidence for the level was observed.

[c]To convert to differential cross section in μb/sr, divide the intensity value quoted by (1) 10.28 for (α,t) and (2) 9.15 for (^{3}He,d).

[d]Observed only at 40° and 60°.

[e]Observed only at 45° and 75°.

[f]Entries without parentheses are from Ref. 13. Those with parentheses are tentative assignments from the present study.

[g]Tentative assignments provided in Ref. 25.

measurements were analyzed to check the elemental purity of the target. These measurements were performed using a beam of 14.7 MeV protons from the Princeton University cyclotron, and the reaction products were analyzed with the Q3D magnetic spectrometer. Several light- and medium-mass impurities were found, and effects due to these contaminants were easily identified as very broad peaks in the spectra. Figure 4 show the ^{226}Ra(p,p′) spectrum obtained at 90°. Using the tail of the elastic peak as an upper limit, the maximum amount of heavy-element contamination of various masses is estimated to be <2% for $A\sim208$, <1% for $A\sim197$, <0.6% for $A\sim181$, <0.1% for $A\sim169$, and <0.06% for $A\sim150$. Furthermore, all the inelastic excitations can be accounted for as levels in ^{226}Ra (Ref. 25). On the basis of these data, virtually no interference from (α,t) or (^{3}He,d) reactions on daughter or other heavy-element impurities is expected.

B. Experimental level scheme for ^{227}Ac

The results of the ^{226}Ra(α,t)^{227}Ac and ^{226}Ra(^{3}He,d)^{227}Ac reactions show that most of the known levels in ^{227}Ac were populated, although in some cases there were unresolved, closely spaced levels. In addition, 11 new levels have been located in the energy region below 1.1 MeV. This information is summarized in Table I and in Fig. 5.

The level assignments adopted in the present work are shown on the spectrum of Fig. 1 and in Table I. Although Nilsson quantum numbers have been used for labeling purposes, note that these labels are only approximate if an octupole deformation exists.

The $\frac{3}{2}^-[532]$, $\frac{3}{2}^+[651]$, $\frac{1}{2}^-[530]$, and $\frac{1}{2}^+[660]$ bands were assigned previously,[13] and the spectroscopic strengths measured in this work provide confirmation for the first three of these bands. The previously assigned

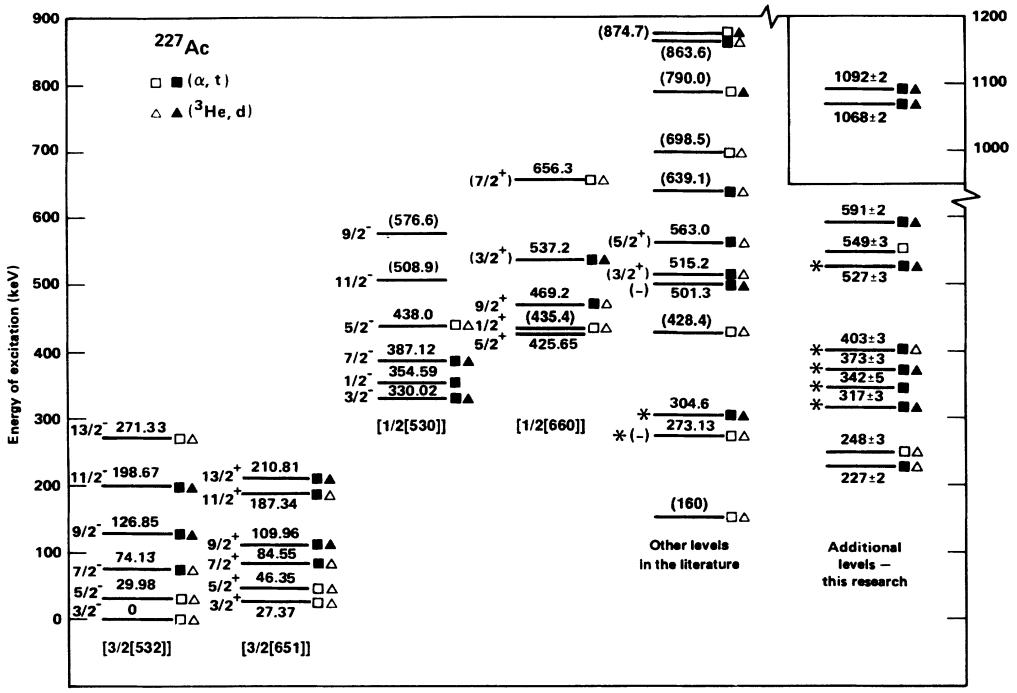

FIG. 5. The level diagram of ^{227}Ac. New levels observed in the present study are shown to the right and are quoted with energies which are the weighted average of the two independently measured values given in Table I. Open squares or triangles indicate either that the levels is part of an unresolved multiplet or that it is only weakly populated ($<2\mu$b at 70°). Parentheses indicate uncertain spin-parity assignments, but the spin value given is among previously established and acceptable possibilities. The levels preceded by asterisks have been tentatively assigned to the $\frac{5}{2}^{\pm}$ parity doublet (see Fig. 8). The 591-keV level is excited strongly in the charged-particle studies and can be reasonably interpreted as the $\frac{13}{2}$ state arising from the $\frac{1}{2}^{+}$[660] configuration. See text for further detail.

band members based on the $\frac{1}{2}^{+}$[660] hole state are expected to be weakly populated in stripping reactions, as we observe. For this band, the largest spectroscopic strength should be located in the previously unassigned $I=\frac{13}{2}$ member. A tentative assignment of this member to the newly observed level at 591 keV has been made, since the excitation energy and cross sections are close to the expected values (see Sec. IV).

It has been pointed out[26] that either the state at 515.2 keV or the state at 537.2 keV might be the $\frac{3}{2}^{+}$ member of the $\frac{1}{2}^{+}$[660] band. Theory suggests that an additional $\frac{3}{2}^{+}$ band head should be observed in this energy region populated with a larger cross section than the $\frac{3}{2}^{+}$ member of the $\frac{1}{2}^{+}$[660] band. The rationale in this study has been to test the existing assignments.[13] Accordingly, the $\frac{3}{2}^{+}$ member of the $\frac{1}{2}^{+}$[660] band has been associated with the 537.2 keV states.

There are only three levels below ~1 MeV remaining unassigned that have reasonably large or moderate cross sections. These are at 317, 373, and 527 keV. From a comparison of expected and observed cross sections, these have been placed in tentatively assigned $\frac{5}{2}^{-}$[523] and $\frac{5}{2}^{+}$[642] bands (see Fig. 8) for which the band heads are the previously known levels at 273.13 keV and 304.6 keV, respectively. The latter band also includes the newly observed but weakly populated levels at 342 and 403 keV. The energy spacings within these bands are reasonable, and the comparison of observed and predicted strengths used in these suggested assignments will be presented.

C. Determination of spectroscopic strengths

The differential cross section for a stripping reaction with an even-even target, exciting a state with spin I, is given by

$$d\sigma/d\Omega=(2I+1)NS_{jl}\phi_l(\theta)\ , \tag{1}$$

where N is a normalization factor, S_{jl} is the spectroscopic factor, $j=I$, and $\phi_l(\theta)$ is the intrinsic single-particle cross section for the transfer of a nucleon with orbital angular momentum l. The spectroscopic factor contains all the nuclear-structure information about the final states populated in the reaction. With reference to Satchler,[27] the spectroscopic factor is expressed as

$$S_{jl}=\frac{2}{2j+1}\left[\sum_{\Omega} a_{\Omega}C_{jl\Omega}U_{\Omega}\right]^2\ , \tag{2}$$

where $C_{jl\Omega}$ are the spherical amplitudes of the Nilsson states, $|N\Omega\rangle$; a_{Ω} are the mixing amplitudes, and U_{Ω} are pairing factors. In studies of deformed nuclei, the quanti-

ty $(\sum_\Omega a_\Omega C_{jl\Omega} U_\Omega)^2$ is often called the nuclear-structure factor.

The computer code DWUCK (Ref. 21) was used to calculate the various single-particle cross sections, $\phi_l(\theta)$, necessary to describe the (α,t) and (^{3}He,d) reactions on ^{226}Ra. The optical-model parameters were taken from Ref. 22. Finite-range and nonlocal corrections were not included in the calculations. The DWBA cross sections were calculated for excitation energies of 0 and 500 keV, and a linear interpolation was used to determine the cross sections for other excitation energies. A normalization factor of $N=6.14$ for the (^{3}He,d) reaction has been adopted based on observations over a wide range of rare-earth and actinide nuclei.[28,29] The normalization factor for the (α,t) reaction is not well established, and the value needed to reproduce known spectroscopic factors varies widely with small changes in the optical parameters used for the DWBA calculations. To obtain $N_{(\alpha,t)}$, the ratio $K=N_{(\alpha,t)}/N_{(^3\mathrm{He,d})}$ was evaluated by using Eq. (1) and measured cross sections for the $\frac{9}{2}^-$ (127 keV) and $\frac{13}{2}^+$ (211 keV) states. This ratio depends on the parameters used for the DWBA calculations but, if the two states have been correctly assigned, it should be independent of any other nuclear structure variables. Using the cross section measured at the three scattering angles for each reaction yields nine ratios, and these are shown for comparison in Fig. 6. Excellent consistency is observed among all the data points, which have the weighted-average value $K=17\pm2$. Given this result and the assumption that $N_{(^3\mathrm{He,d})}=6.14$, a value of 104 is obtained for $N_{(\alpha,t)}$.

In Table II, the nuclear-structure factors obtained from the (α,t) data are compared with theoretical values to be discussed in the next section. The experimental results shown are weighted averages of values from all the angles. The (α,t) data were used for this purpose, rather than the (^{3}He,d) results, because the inherently better resolution permitted intensities for more levels to be extracted from the spectra.

III. DISCUSSION

A. Energy level systematics and model comparisons

An energy-level diagram for protons at $\beta_2=0.17$ and $\beta_4=0.11$ is shown in Fig. 7 as a function of the octupole-deformation parameter β_3. This figure was obtained by plotting the results published in Ref. 20. The reflection symmetric quadrupole-deformed orbitals ($\beta_3=0.0$) are given at the left of the diagram and are labeled by the usual asymptotic quantum numbers $\Omega[Nn_z\Lambda]$. For $\beta_3=0.0$, the 89th proton in ^{227}Ac is predicted to occupy the $\frac{1}{2}^-[530]$ orbital. This orbital would be the ground state of ^{227}Ac, if the nucleus were reflection symmetric. However, the ground state band of ^{227}Ac has been assigned to the $\frac{3}{2}^-[532]$ orbital, which is $\sim$0.5 MeV below the predicted ground state for a pure quadrupole shape. The calculated ground-state spin depends on the parameters used in the single-particle potential. For example, if one uses a Nilsson calculation with the parameters of

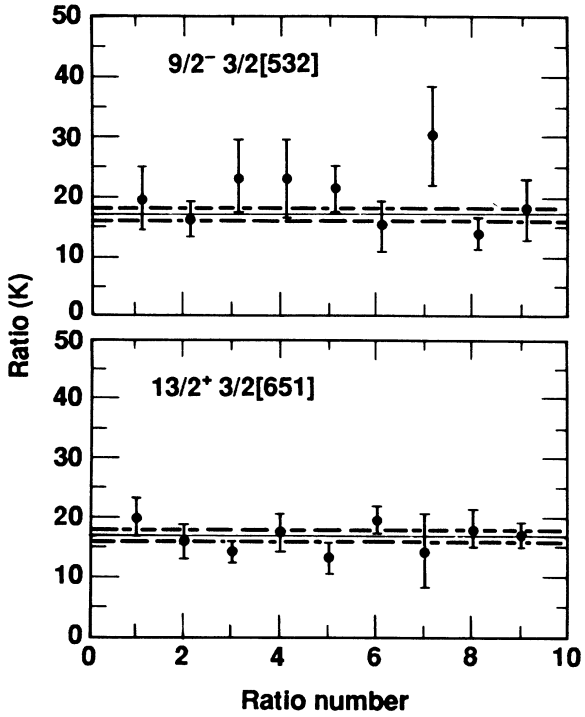

FIG. 6. Experimentally determined ratio of the charged-particle normalization factors [$K=N_{(\alpha,t)}/N_{(^3\mathrm{He,d})}$]. The data are shown for the $\frac{9}{2}^-$ member of the $I^\pi=\frac{3}{2}^-$ ground state and for the $\frac{13}{2}^+$ state built on the $I^\pi=\frac{3}{2}^+$ band head at 27.4 keV. Experimental ratios are plotted as solid points with error bars. The weighted average (solid line) as well as the associated error of the data (broken line) are shown for comparison. The weighted average from both sets of data gives $K=17\pm2$. See text for further discussion.

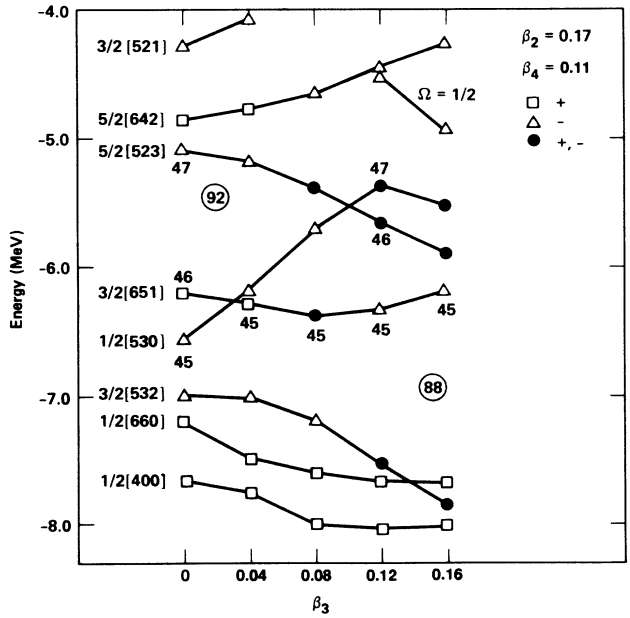

FIG. 7. Nilsson energy-level diagram for protons as a function of the octupole-deformation parameter, β_3. The shape and shading of the points roughly indicate the parity purity of each orbital at the appropriate value of the octupole deformation: an open square or triangle indicates nearly pure + or − parity, respectively; a dark circle indicates that the orbital is highly parity mixed.

TABLE II. Comparison between the experimental[a] and theoretical nuclear structure factors for states in ^{227}Ac.

			$(\sum aC_{jl}U)^2$					$(\sum aC_{jl}U)^2$	
E[b]	I	Expt.[c]	Theory sym.	Theory asym.	E[b]	I	Expt.[c]	Theory sym.	Theory asym.
		$\frac{1}{2}^+[660]$					$\frac{1}{2}^-[530]$		
435*	$\frac{1}{2}$	<0.20	0.0002	0.0600	355	$\frac{1}{2}$	0.12(4)	0.0146	0.0433
537	$\frac{3}{2}$	0.12(3)	0.0003	0.0050	330	$\frac{3}{2}$	0.20(3)	0.1111	0.1592
426*	$\frac{5}{2}$	<0.02	0.0040	0.0114	438*	$\frac{5}{2}$	<0.14	0.0017	0.0052
656*	$\frac{7}{2}$	<0.011	0.0001	0.006	387	$\frac{7}{2}$	0.51(3)	0.5110	0.2007
469	$\frac{9}{2}$	0.032(5)	0.0087	0.0121	577	$\frac{9}{2}$	0.11(5)	0.1648	0.1347
?	$\frac{11}{2}$		0.0000	0.0003	(509)	$\frac{11}{2}$		0.0743	0.0600
591	$\frac{13}{2}$	0.53(9)	0.4188	0.0276	?	$\frac{13}{2}$			
		$\frac{3}{2}^+[651]$					$\frac{3}{2}^-[532]$		
27*	$\frac{3}{2}$	<0.017	0.0002	0.0190	0	$\frac{3}{2}$	0.012(3)	0.0040	0.0002
46	$\frac{5}{2}$	0.009(4)	0.0200	0.0059	30*	$\frac{5}{2}$	<0.051	0.0368	0.0256
85	$\frac{7}{2}$	0.033(6)	0.0006	0.0036	74	$\frac{7}{2}$	0.087(7)	0.0410	0.0262
110	$\frac{9}{2}$	0.12(1)	0.0659	0.0538	127	$\frac{9}{2}$	0.76(7)	0.9388	0.3364
187	$\frac{11}{2}$	0.14(3)	0.0085	0.0053	199	$\frac{11}{2}$	0.06(2)	0.0246	0.0015
211	$\frac{13}{2}$	2.1(1)	1.5468	0.7005	271*	$\frac{13}{2}$	<0.076		
		$\frac{5}{2}^+[642]$					$\frac{5}{2}^-[523]$		
305	$\frac{5}{2}$	0.017(7)	0.0019	0.0012	273*	$\frac{5}{2}$	<0.067	0.0027	0.0042
342	$\frac{7}{2}$	0.06(2)	0.0026	0.0030	317	$\frac{7}{2}$	0.18(2)	0.0216	0.0949
403	$\frac{9}{2}$	0.08(1)	0.0041	0.0125	373	$\frac{9}{2}$	0.73(4)	0.6670	0.3807
?	$\frac{11}{2}$		0.0050	0.0004	?	$\frac{11}{2}$		0.0117	0.0365
527	$\frac{13}{2}$	0.58(9)	0.2879	0.2016	?	$\frac{13}{2}$			

[a]Obtained from a weighted average of the (α,t) data only.

[b]An asterisk indicates that the spectroscopic factor is derived from the intensity of an unresolved peak. At best, such values are upper limits.

[c]A number in parentheses is the statistical error in the least significant digit quoted.

Lamm[30] instead of the Saxon-Woods calculation,[20] the $\frac{3}{2}^+[651]$ orbital is expected to be the ground state. Although there is uncertainty of this kind in the theoretical level ordering, none of the calculations optimized for a broad range of masses predicts that the 89th proton orbital at $\beta_2=0.17$ and $\beta_3=0.0$ is the $\frac{3}{2}^-[532]$ orbital.

When static octupole deformation is included, the octupole-deformed intrinsic orbitals are degenerate parity doublets. The energy of each doublet as a function of octupole deformation is shown in Fig. 7. Only Ω remains a good quantum number, and the orbitals are labeled by Ω and by a number that notes their position in the static potential well.

A value of $\beta_3=0.1$ has been suggested by Leander and Sheline[9] for ^{227}Ac. At this octupole deformation, the calculated energy sequence is in agreement with the experimentally determined energies for the $\frac{3}{2}^{\pm}$, $\frac{5}{2}^+$, and $\frac{1}{2}^{\pm}$ intrinsic levels. Furthermore, the parity-mixed orbital number 45, for deformation $\beta_3=0.1$, has $\Omega=\frac{3}{2}$ and is predominantly negative in parity (see Fig. 7). Thus, the $\frac{3}{2}^-$ member should be the ground state and the $\frac{3}{2}^+$ member should be the first excited state. This is observed experimentally. The 46th ($\Omega=\frac{5}{2}$) and 47th ($\Omega=\frac{1}{2}$) orbitals each have comparable mixtures of different-parity Nilsson orbitals and, therefore, the parity member that lies lower in energy cannot be predicted from Fig. 7 alone.

Recently, Leander and Chen[31] have used a nonadiabatic reflection-asymmetric rotor model to calculate the structure of the low-lying levels in ^{227}Ac. Coriolis and parity decoupling from quadrupole and octupole deformations, respectively, were both taken into account.

The Hamiltonian used in these calculations is

$$H=H_{\rm sp}+H_{\rm rot}+H_{\rm pair}+\tfrac{1}{2}\epsilon_0(1-P)\ ,$$

where $H_{\rm sp}$ is a single-particle Hamiltonian solved for a nonzero value of static octupole deformation ($\beta_3\neq 0$). The terms $H_{\rm rot}$ and $H_{\rm pair}$ take account of the usual nuclear-rotational and pairing dynamics, and the last term causes parity splitting where P is the parity of the core. The value of ϵ_0 is chosen to reproduce the splitting between the states of opposite parity in the neighboring even-even nuclei (in ^{227}Ac, ϵ_0 was taken as the average of the values in ^{226}Ra and ^{228}Th: 290 keV).

Using this model, Leander and Chen have calculated level energies for the $K=\frac{3}{2}^{\pm}$ and $\frac{1}{2}^{\pm}$ parity doublet bands

and nuclear-structure factors for the $K=\frac{3}{2}^{\pm}$ bands and compared them with the experimental results of this study.[31] The deformation parameters used for ^{227}Ac are $\beta_2=0.168$, $\beta_3=0.1$, $\beta_4=0.094$, $\beta_5=0.1$, and $\beta_6=0.0052$. Each of these parameters is approximately the mean of the appropriate equilibrium values of the even-even neighbors except β_3, which is expected to have a larger value for ^{227}Ac.

The results of a more recent and detailed calculation[26] of the level structure for ^{227}Ac using the Leander-Chen model are shown in Fig. 8. These results qualitatively reproduce the level ordering observed. Although absolute values of the energy splittings are not well reproduced, the signs of the splitting of the parity doublets are always correctly predicted. The discrepancies between experiment and theory for the $K=\frac{1}{2}^{\pm}$ parity doublet bands may be caused by the fact that the decoupling parameter for the $\frac{1}{2}^-$ band predicted by theory is -2.8 whereas experimentally it is -2.16, and for the $\frac{1}{2}^+$ band the theoretical value is 4.1 while the experimental value is 5.3. Using the many-body wave functions,[4] one does somewhat better in understanding the decoupling parameters of these bands. For the $\frac{1}{2}^+$ band, one obtains a value of 4.95 and, for the $\frac{1}{2}^-$ band, -1.75. The experimental decoupling parameters were determined by taking all of the energy levels of the $K=\frac{1}{2}^{\pm}$ bands into account.[32]

B. Experimental nuclear-structure factors and the use of nuclear-reaction spectroscopy to test models for ^{227}Ac

Using single-nucleon transfer reactions, one can assign specific bands in reflection-symmetric deformed nuclei. This is because the cross section for populating each member of a rotational band can be calculated with reasonable accuracy. The addition of octupole deformation to the nuclear potential affects the wave functions of the states, and hence the spectroscopic strengths for populating members of the rotational band. Thus as a test of the existence of octupole deformation in ^{227}Ac, one can compare the nuclear-structure factors of the present work with those predicted for various magnitudes of β_3.

Data from the present work are compared with two sets of theoretically calculated structure factors. The first set was obtained from a reflection-symmetric Nilsson model calculation with pairing and Coriolis effects included. The parameters used for the Nilsson calculation were $\kappa=0.058$, $\mu=0.646$, $\beta_2=0.17$, $\beta_3=0.0$, and $\beta_4=0.09$. Emptiness factors, U^2_Ω, for the various orbitals in the ^{226}Ra target were estimated from the observed excitation energies in ^{227}Ac, assuming the Fermi surface for ^{227}Ac was at the position of the $\frac{3}{2}^-[532]$ orbital, and that for ^{226}Ra it was ~ 250 keV lower. The pairing strength parameter was $\Delta=0.79$ MeV. Coriolis mixing calculations were performed for both the positive and negative parity bands. For positive parity levels, the calculations included all rotational bands based on the spherical $i_{13/2}$ level. For $K=\frac{7}{2}$ and greater, the bandhead energies were estimated from harmonic oscillator calculations and systematics. For the three experimentally known bands, a least-squares fit was made to all of the levels of the $\frac{3}{2}^+[651]$ band, to the $I=\frac{5}{2}$ and $\frac{13}{2}$ members of the $\frac{5}{2}^+[642]$ band, and to the $I=\frac{5}{2}$, $\frac{9}{2}$, and $\frac{13}{2}$ members of the $\frac{1}{2}^+[660]$ band. Variables in the calculation were the unperturbed bandhead energies of the three bands, a common moment of inertia, and a decoupling parameter; the Coriolis matrix elements were fixed at 50% of their theoretical values.

For the negative-parity levels, the Coriolis mixing calculations were performed including the three experimentally observed bands plus $K=\frac{7}{2}$ and $\frac{9}{2}$ bands from the $h_{9/2}$ spherical state with estimated excitation energies. A least-squares fit was made to all of the (negative-parity) experimental levels shown in Fig. 8 except the $I=\frac{9}{2}$ and $\frac{11}{2}$ members of the $K^\pi=\frac{1}{2}^-$ band. Variables in the calculation were treated just as in the calculation for positive-parity bands.

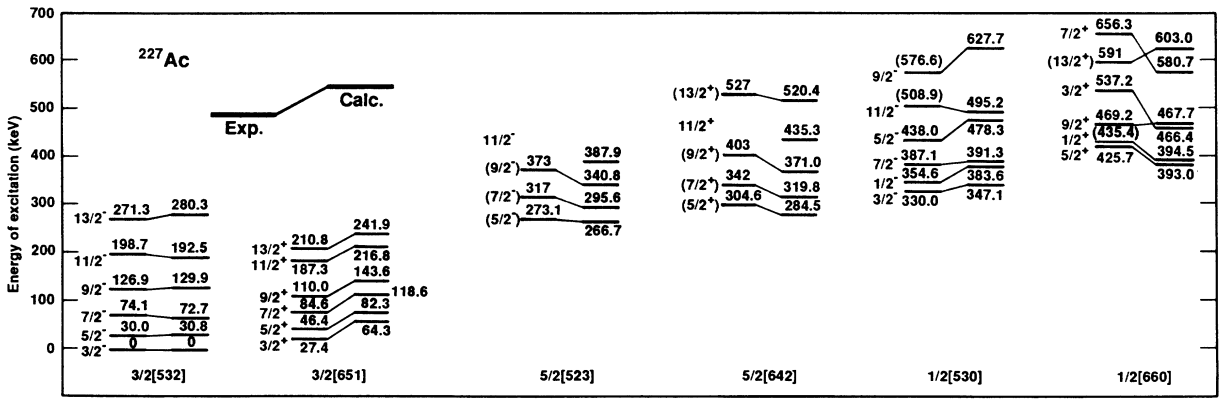

FIG. 8. Comparison of the experimental energy levels of ^{227}Ac with those from the nonadiabatic asymmetric rotor model of Leander and Chen. The calculated energies (right) are connected by a thin line with their presumed measured values (left). Parentheses around a spin-parity value indicate that the spin-parity assignment is very tentative and is suggested solely on the basis of energy and cross section comparisons (see also Fig. 9). Spin-parity values not in parentheses are taken from Ref. 13.

The second set of nuclear-structure factors was predicted by the adiabatic reflection-asymmetric rotor model of Leander and Chen. There is no reduction of Coriolis matrix elements in this calculation. Inclusion of the standard reduction factor would lower the calculated structure factors for the $\frac{13}{2}^+$ level at 211 keV and $\frac{9}{2}^-$ level at 127 keV substantially, as well as change other structure factors. Values for the $K^\pi=\frac{3}{2}^\pm$ bands are from Ref. 31, while those for the $\frac{5}{2}^\pm$ and $\frac{1}{2}^\pm$ bands were obtained more recently.[26] The two theoretical sets are compared with experimental values in Table II and Fig. 9.

Before commenting on these results, some general remarks should be made. First, there have been no arbitrary adjustments or renormalization in either the measured or calculated results. The comparisons involve absolute values. Second, the experimental values have been extracted from the measured cross sections assuming the reaction process is described by a single-step DWBA process. It is well known, however, that multistep processes in the reaction mechanism can be significant, particularly for weakly populated members of bands that have a strongly populated member.[33,34] Since inelastic-scattering events in the entrance and exit channels can effectively transfer some strength from one band member to another, the net result is that the strengths of weakly populated levels are often affected significantly. Therefore, it is unrealistic to compare calculated and measured spectroscopic strengths for levels populated less than 10–20% of that for the most strongly populated members of the same band. In the following discussion of the various models, consideration should be restricted to the half dozen or so levels for which the strengths shown in Fig. 9 are reasonably large (e.g., larger than ~0.2).

From Fig. 9 it is seen that a better overall description of the observed spectroscopic strengths is obtained with

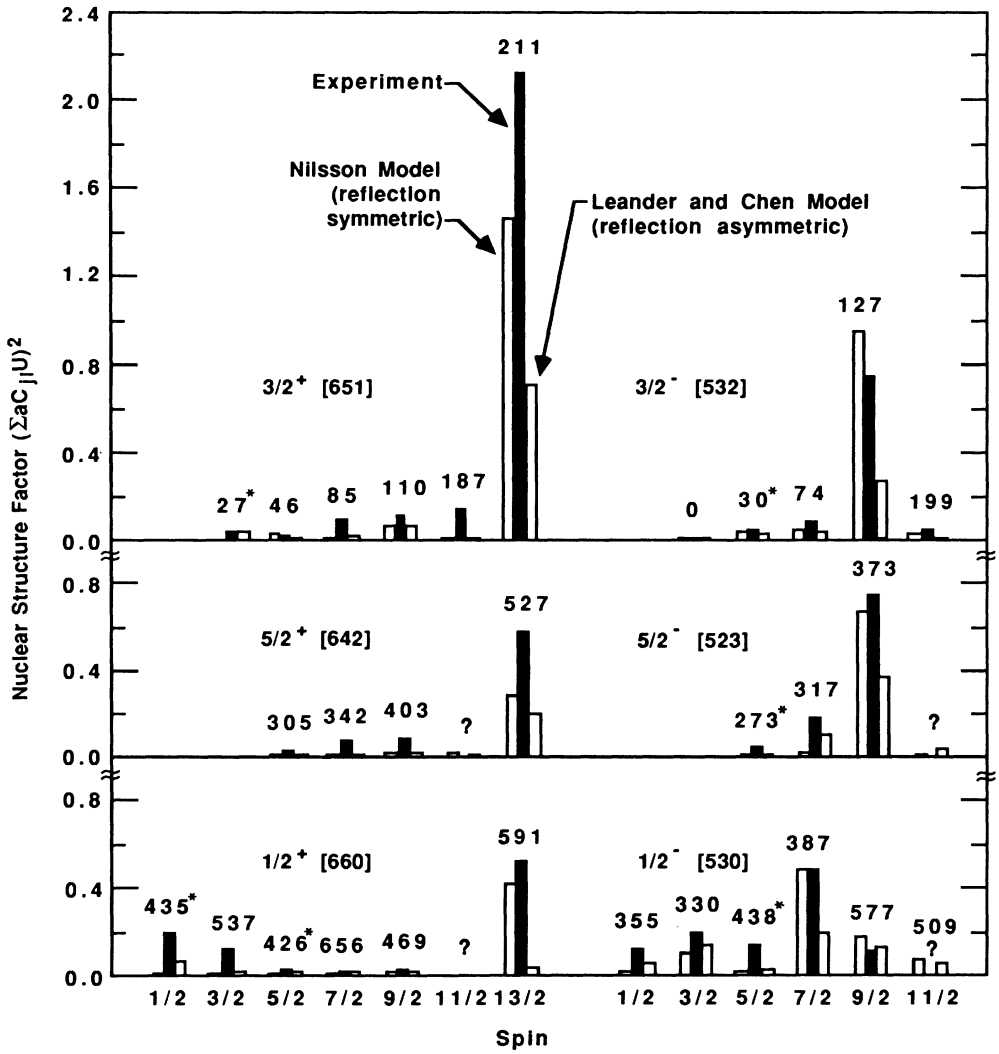

FIG. 9. The experimental and calculated structure factor, $(\sum aC_{ji}U)^2$, for states in ^{227}Ac. The solid bars are the experimental results of this research; the reflection symmetric Nilsson model calculations are the open bars to the left; the reflection asymmetric Leander and Chen calculations are the open bars to the right. The proposed experimental energies are noted above the results for each state. An asterisk (*) shows that some or all of the measured strength may be due to another state(s) which cannot be experimentally resolved; a question mark notes that no assignment has been made on the basis of this research.

the Nilsson model for $\beta_3=0$, with Coriolis mixing effects included. The adiabatic reflection-asymmetric rotor model of Leander and Chen underestimates most of the largest strengths by an approximately constant factor of 2–3 (the excellent agreement shown in Ref. 31 was obtained by renormalizing the experimental strengths to agree with the calculated values).

C. Alternate model interpretations for ^{227}Ac

In many-body calculations[4] for ^{227}Ac, a ground-state parity doublet of $\frac{3}{2}^-$, $\frac{3}{2}^+$ was obtained. The calculated splitting of the doublet is 23 keV, which is in extremely good agreement with the experimental value of 27.4 keV. This is substantially better than the value of 64.3 keV that one gets with the static octupole model. This calculation also predicted a $\frac{5}{2}^-$, $\frac{5}{2}^+$ parity doublet having a splitting of 18 keV, with the bandhead at 470 keV. In addition (as noted in Sec. IV A), this calculation gives rather good values of the decoupling parameters in the $\frac{1}{2}^+$ and $\frac{1}{2}^-$ bands. These calculations do not provide predictions of the spectroscopic strengths for comparison with the transfer reaction data.

Recently, Piepenbring[32] extended a multiphoton octupole model with $\beta_3=0$ to odd-mass deformed nuclei and made calculations for ^{223}Ac, ^{225}Ac, and ^{227}Ac. Although no specific results are given for ^{227}Ac, it is interesting to note that for ^{223}Ac and ^{225}Ac the model gives the correct parity doublets and also predicts enhanced $E1$ transition probabilities that vary from band to band and from isotope to isotope. The multiphoton model further predicts the appropriate ground state for both ^{223}Ac and ^{225}Ac when some of the model parameters are adjusted. Finally, an alpha clustering model[35] has also been proposed, but thus far, it has only been applied to even-even nuclei. Predicted spectroscopic strengths are not yet available for these models.

IV. SUMMARY AND CONCLUSIONS

This single-proton-transfer study was undertaken to measure the differential cross sections and determine the energy levels of ^{227}Ac, in order to see if these observables would yield an improved understanding of the nuclear structure. Most of the previously observed states were seen in this research and some additional levels were found. Bands with $K^\pi=\frac{5}{2}^+$ and $K^\pi=\frac{5}{2}^-$ have been tentatively assigned.

Earlier papers have shown that octupole effects provide a better description of certain nuclear properties, such as level ordering and spacing, decoupling parameters, magnetic moments, etc. However, the present experiment shows that the spectroscopic strengths for single-proton stripping reactions are in better agreement with predictions of the Nilsson model with no octupole deformation. Although the model of Leander and Chen can reproduce the correct level order and account for the observed parity doublets, the calculated nuclear-structure factors for most of the important strongly populated levels tend to be too small by a factor of 2–3.

The energy resolution obtained in the (α,t) measurements is comparable to the best obtained in any single-proton transfer studies of heavy nuclei and is limited largely by effects due to thickness of the target and its backing. It is unlikely that improved charged-particle data would alter the general conclusions that have already been made on the basis of the strongest peaks in the spectra. However, additional experiments that could test the tentative spin-parity and configuration assignments for the weaker states would provide a more confident evaluation of the applicability of these models.

ACKNOWLEDGMENTS

We wish to thank George Leander and Yong-Shou Chen for sending us their calculations for ^{227}Ac prior to publication. We also wish to thank George Leander for carefully reading our manuscript and making valuable suggestions. This study was supported by the National Science Foundation under Contract PHY-8605032 with Florida State University and performed under the auspices of the U.S. Department of Energy by the Lawrence Livermore National Laboratory under Contract W-7405-ENG-48. Financial support for the McMaster University Tandem Accelerator Laboratory and for an operating grant to one of the authors (D.G.B.) was provided by the National Sciences and Engineering Research Council of Canada.

*Permanent address: Mechanical Engineering Department, Lawrence Livermore National Laboratory, Livermore, CA 94550.

†Permanent address: Nuclear Research Building, Florida State University, Tallahassee, FL 32306.

[1]F. Stephens, F. Asaro, and I. Perlman, Phys. Rev. **96**, 1568 (1954); **100**, 1543 (1955).

[2]K. Alder, A. Bohr, T. Huus, B. Mottelson, and A. Winther, Rev. Mod. Phys. **28**, 432 (1956).

[3]A. Bohr and B. R. Mottelson, *Nuclear Structure* (Benjamin, Reading, Massachusetts, 1975), Vol. II.

[4]R. R. Chasman, Phys. Lett. **96B**, 7 (1980).

[5]P. Möller and J. R. Nix, Nucl. Phys. **A361**, 117 (1981).

[6]G. A. Leander, R. K. Sheline, P. Möller, P. Olanders, I. Ragnarsson, and A. J. Sierk, Nucl. Phys. **A388**, 452 (1982).

[7]W. Nazarewicz *et al.*, Nucl. Phys. **A429**, 269 (1984).

[8]R. R. Chasman, J. Phys. (Paris) Colloq. Suppl. **45**, C6-167 (1984).

[9]G. A. Leander and R. K. Sheline, Nucl. Phys. **A413**, 375 (1984).

[10]P. Bonche, P. H. Heenen, H. Flocard, and D. Vautherin, Phys. Lett. **175B**, 387 (1986).

[11]R. R. Chasman, Phys. Lett. **175B**, 254 (1986).

[12]I. Ahmad *et al.*, Phys. Rev. Lett. **49**, 1758 (1982).

[13]R. K. Sheline and G. Leander, Phys. Rev. Lett. **51**, 359 (1983).
[14]I. Ragnarsson, Phys. Lett. **130B**, 353 (1983).
[15]C. Maples, Nucl. Data **22**, 275 (1977).
[16]W. Teoh, R. D. Connor, and R. H. Betts, Nucl. Phys. **A319**, 122 (1979).
[17]I. Aniĉin, I. Bikit, C. Girit, H. Güven, W. D. Hamilton, and A. A. Yousif, J. Phys. G **8**, 369 (1982).
[18]T. Ishii *et al.*, Nucl. Phys. **A444**, 237 (1985).
[19]B. Elbek and P. O. Tjøm, in *Advances in Nuclear Physics,* edited by M. Baranger and E. Vogt (Plenum, New York, 1969), Vol. 3, p. 259.
[20]R. R. Chasman, Phys. Rev. C **30**, 1753 (1984).
[21]P. D. Kunz (private communication).
[22]T. W. Elze and J. R. Huizenga, Phys. Rev. C **1**, 328 (1970).
[23]W. Stöffl (private communication).
[24]J. Wilhelmy (private communication).
[25]*Table of Isotopes,* edited by C. M. Lederer and V. S. Shirley (Wiley, New York, 1978).
[26]G. A. Leander and Y. S. Chen (private communication).
[27]G. R. Satchler, Ann. Phys. **3**, 275 (1958).
[28]O. Straume, G. Løvhøiden, and D. G. Burke, Nucl. Phys. **A226**, 390 (1976).
[29]T. W. Elze and J. R. Huizenga, Z. Phys. A **272**, 119 (1975).
[30]Inger-Lena Lamm, Nucl. Phys. **A125**, 504 (1969).
[31]G. A. Leander and Y. S. Chen, Phys. Rev. C **35**, 1145 (1987).
[32]R. Piepenbring, Z. Phys. A **323**, 341 (1986).
[33]R. J. Ascuitto, C. H. King, L. J. McVay, and B. Sørensen, Nucl. Phys. **A226**, 454 (1974).
[34]T. F. Thorsteinsen, J. S. Vaagen, G. Løvhøiden, D. G. Burke, and E. R. Flynn, Phys. Lett. **93B**, 223 (1980).
[35]F. Iachello and A. D. Jackson, Phys. Lett. **108B**, 151 (1982).